Continuous Theory of Active Matter Systems with Metric-Free Interactions

Anton Peshkov,[1,2,6] Sandrine Ngo,[1,6] Eric Bertin,[3,6] Hugues Chaté,[1,2,6] and Francesco Ginelli[4,5]

[1]*Service de Physique de l'Etat Condensé, CEA-Saclay, 91191 Gif-sur-Yvette, France*
[2]*LPTMC, CNRS-UMR 7600, Université Pierre et Marie Curie, 75252 Paris, France*
[3]*Laboratoire de Physique, Université de Lyon, ENS Lyon, CNRS, 46 Allée d'Italie, 69007 Lyon, France*
[4]*Istituto dei Sistemi Complessi, CNR, via dei Taurini 19, I-00185 Roma, Italy*
[5]*SUPA, Institute for Complex Systems and Mathematical Biology, King's College, University of Aberdeen, Aberdeen AB24 3UE, United Kingdom*
[6]*Max Planck Institute for the Physics of Complex Systems, Nothnitzer Str. 38, 01187 Dresden, Germany*
(Received 30 March 2012; published 28 August 2012)

We derive a hydrodynamic description of metric-free active matter: starting from self-propelled particles aligning with neighbors defined by "topological" rules, not metric zones—a situation advocated recently to be relevant for bird flocks, fish schools, and crowds—we use a kinetic approach to obtain well-controlled nonlinear field equations. We show that the density-independent collision rate per particle characteristic of topological interactions suppresses the linear instability of the homogeneous ordered phase and the nonlinear density segregation generically present near threshold in metric models, in agreement with microscopic simulations.

DOI: 10.1103/PhysRevLett.109.098101 PACS numbers: 87.10.Ca, 05.20.Dd, 05.65.+b, 87.18.−h

Collective motion is a central theme in the emerging field of active matter studies [1]. For physicists, the interest largely lies in the nontrivial cases where the emergence of collective motion can be seen as an instance of spontaneous symmetry breaking out of equilibrium: without leaders, guiding external fields, or confinement by boundaries, large groups inside of which an "individual" can only perceive local neighbors are able to move coherently. After this was realized in the seminal papers of Vicsek *et al.* [2] and Toner and Tu [3], much progress has been recorded in the physics community [1,4], alongside continuing modeling work in ethology and biology [5,6].

Most models consist of self-propelled particles interacting with neighbors defined to be those particles within some finite distance [7]. Among those "metric models," that introduced by Vicsek *et al.* [2] is arguably the simplest: in the presence of noise, point particles move at constant speed, aligning ferromagnetically with others currently within unit distance. The study of the Vicsek model has revealed rather unexpected behavior. Of particular importance in the following is the emergence of phase segregation, under the form of high-density high-order traveling bands [8], in a large part of the orientationally ordered phase bordering the onset of collective motion, relegating further the spatially homogeneous fluctuating phase treated by Toner and Tu. Similar observations of density segregation were made for important variants of the Vicsek model, such as polar particles with nematic alignment [9] (self-propelled rods) or the active nematics model of Refs. [10,11]. The genericity of these observations has been confirmed, in the Vicsek case, by the derivation and analysis of continuous field equations [12,13] (see also Refs. [14,15]). It was shown in particular that the homogeneous ordered solution is linearly unstable near onset, and that solitary wave structures akin to the traveling bands, arise at the nonlinear level.

Even though metric interaction zones are certainly of value in cases such as shaken granular media [16,17] and motility assays [18,19] where alignment arises mostly from inelastic collisions, it has been argued recently [20–22] that they are not realistic in the context of higher organisms such as birds, fish, or pedestrians, whose navigation decisions are likely to rely on interactions with neighbors defined using metric-free, "topological" criteria. Statistical analysis of flocks of hundreds to a few thousand of individuals revealed that a typical starling interacts mostly with its 7 or 8 closest neighbors, regardless of the flock density [20]. The realistic, data-based, model of pedestrian motion developed by Moussaid *et al.* relies on the "angular perception landscape" formed by neighbors screening out others [21].

At a more theoretical level, the study of the Vicsek model with Voronoi neighbors [23] (those whose associated Voronoi cells form the first shell around the central cell) has shown that metric-free interactions are relevant at the collective scale: in particular, the traveling bands mentioned above disappear, leaving only a Toner-Tu-like phase. Below, we show that the introduction of Voronoi neighbors suppresses the density-segregated phase in other variants of the Vicsek model. In spite of the recognized importance of metric-free interactions, no continuous field equations describing the above models are available which would help put the above findings on firmer theoretical ground.

In this Letter, starting from Vicsek-style microscopic models with Voronoi neighbors, we derive nonlinear field equations for active matter with metric-free interactions using a kinetic approach well controlled near the onset of orientational order. We show that the density-independent collision rate per particle characteristic of these systems suppresses the linear instability of the homogeneous ordered phase and the nonlinear density segregation in agreement with microscopic simulations. We finally discuss the consequences of our findings for the relevance of metric-free interactions.

Let us first stress that with metric-free interactions, say with Voronoi neighbors, the tenet of the Boltzmann equation approach [24]—the assumption that the system is dilute enough so that it is dominated by binary collisions—is never justified since, after all, a particle is constantly interacting with almost the same number of neighbors. Here, instead, we introduce an effective interaction rate per unit time, which renders binary interactions dominant in the small rate limit. Apart from the mathematical convenience, it is not unrealistic to think that the stimulus or response function of superior animals—due to the physical constraints induced by the information processing in various cognitive layers [25]—does not treat visual cues continuously.

Our starting point is thus a Vicsek-style model in which information is processed according to some stochastic rates: N point particles move at a constant speed v_0 on a $L \times L$ torus; their heading θ is submitted to two different dynamical mechanisms, "self-diffusion" and aligning binary "collisions." In self-diffusion, θ is changed into $\theta' = \theta + \eta$ with a probability λ per unit time, where η is a random variable drawn from a symmetric distribution $P_\sigma(\eta)$ of variance σ^2. Aligning "collisions" occur at a rate α_0 per unit time with each Voronoi neighbor. In the small α_0 limit, binary interactions dominate and take place with a rate $\alpha \approx n_2\alpha_0$, where n_2 is the typical number of neighbors. In such collisions θ is changed to $\theta' = \Psi(\theta, \theta_n) + \eta$ where θ_n is the heading of the chosen neighbor and the noise η is also drawn, for simplicity, from $P_\sigma(\eta)$. Isotropy is assumed, namely $\Psi(\theta_1 + \phi, \theta_2 + \phi) = \Psi(\theta_1, \theta_2) + \phi[2\pi]$. For the case of ferromagnetic alignment treated in detail below, $\Psi(\theta_1, \theta_2) \equiv \arg(e^{i\theta_1} + e^{i\theta_2})$. Simulations of our stochastic rule indicate that it shares the same collective properties as the system studied in Ref. [23] (not shown).

The evolution of the one-particle phase-space distribution $f(\mathbf{r}, \theta, t)$ (defined over some suitable coarse-grained scales) is governed by the Boltzmann equation

$$\partial_t f(\mathbf{r},\theta,t) + v_0 \mathbf{e}(\theta)\cdot\nabla f(\mathbf{r},\theta,t) = I_{\rm diff}[f] + I_{\rm coll}[f], \quad (1)$$

where $\mathbf{e}(\theta)$ is the unit vector along θ. The self-diffusion integral is

$$I_{\rm diff}[f] = -\lambda f(\theta) + \lambda \int_{-\pi}^{\pi} d\theta' \int_{-\infty}^{\infty} d\eta P_\sigma(\eta) \times \delta_{2\pi}(\theta' - \theta + \eta) f(\theta'), \quad (2)$$

where $\delta_{2\pi}$ is a generalized Dirac delta function imposing that the argument is equal to zero modulo 2π. In the small rate limit, orientations are decorrelated between collisions ("molecular chaos hypothesis"), and one can write

$$I_{\rm coll}[f] = -\alpha f(\theta) + \frac{\alpha}{\rho(\mathbf{r},t)} \int_{-\pi}^{\pi} d\theta_1 \int_{-\pi}^{\pi} d\theta_2 \times \int_{-\infty}^{\infty} d\eta P_\sigma(\eta) f(\theta_1) f(\theta_2) \times \delta_{2\pi}(\Psi(\theta_1,\theta_2) - \theta + \eta). \quad (3)$$

The main difference with the metric case treated in Ref. [12] is the "collision kernel," which is independent from relative angles and inversely proportional to the local density

$$\rho(\mathbf{r},t) = \int_{-\pi}^{\pi} f(\mathbf{r},\theta,t) d\theta. \quad (4)$$

Note that, in agreement with the basic properties of models with metric-free interactions, Eq. (1), together with the definitions of Eqs. (2)–(4), is left unchanged by an arbitrary normalization of f (and thus of ρ) and thus does not depend on the global density $\rho_0 = N/L^2$. Furthermore, a rescaling of time and space allows us to set $\lambda = v_0 = 1$, a normalization we adopt in the following.

Equations for the hydrodynamic fields are obtained by expanding $f(\mathbf{r}, \theta, t)$ in Fourier series, yielding the Fourier modes $\hat{f}_k(\mathbf{r}, t) = \int_{-\pi}^{\pi} d\theta f(\mathbf{r}, \theta, t) e^{ik\theta}$, where $\hat{f}_k$ and $\hat{f}_{-k}$ are complex conjugates, $\hat{f}_0 = \rho$, and the real and imaginary parts of $\hat{f}_1$ are the components of the momentum vector $\mathbf{w} = \rho\mathbf{P}$ with $\mathbf{P}$ the polar order parameter field. Using these Fourier modes, the Boltzmann equation Eq. (1) yields an infinite hierarchy:

$$\partial_t \hat{f}_k + \frac{1}{2}(\nabla \hat{f}_{k-1} + \nabla^* \hat{f}_{k+1}) = (\hat{P}_k - 1 - \alpha)\hat{f}_k + \frac{\alpha}{\rho}\hat{P}_k \sum_{q=-\infty}^{\infty} J_{kq} \hat{f}_q \hat{f}_{k-q}, \quad (5)$$

where the complex operators $\nabla = \partial_x + i\partial_y$ and $\nabla^* = \partial_x - i\partial_y$ have been used, the binary collision rate α is now expressed in the rescaled units, $\hat{P}_k = \int_{-\infty}^{\infty} d\eta P_\sigma(\eta) e^{ik\eta}$ is the Fourier transform of P_σ, and J_{kq} is an integral depending on the alignment rule Ψ. Below, we specialize to the case of ferromagnetic alignment, for which

$$J_{kq} = \frac{1}{2\pi}\int_{-\pi}^{\pi} d\theta \cos[(q - k/2)\theta]. \quad (6)$$

For $k = 0$ the rhs of Eq. (5) vanishes and one recovers the continuity equation

$$\partial_t \rho + \nabla\cdot\mathbf{w} = 0. \quad (7)$$

To truncate and close this hierarchy, we assume the following scaling structure, valid near onset of polar order, assuming, in a Ginzburg-Landau-like approach, small and slow variations of fields

$$\rho - \rho_0 \sim \epsilon, \quad \hat{f}_k \sim \epsilon^{|k|}, \quad \nabla \sim \epsilon, \quad \partial_t \sim \epsilon. \quad (8)$$

Note that the scaling of space and time is in line with the propagative structure of our system [26]. The lowest order yielding nontrivial, well-behaved equations is ϵ^3: keeping only terms up to this order, equations for $\hat{f}_{k>2}$ identically vanish, while $\hat{f}_2$, being slaved to $\hat{f}_1$, allows us to close the $\hat{f}_1$ equation which reads, in terms of the momentum field $\mathbf{w}$:

$$\partial_t \mathbf{w} + \gamma(\mathbf{w}\cdot\nabla)\mathbf{w} = -\frac{1}{2}\nabla\rho + \frac{\kappa}{2}\nabla\mathbf{w}^2 + (\mu - \xi\mathbf{w}^2)\mathbf{w} + \nu\nabla^2\mathbf{w} - \kappa(\nabla\cdot\mathbf{w})\mathbf{w}. \quad (9)$$

Apart from some higher order terms we have discarded here, this equation has the same form as the one derived in Ref. [12] for metric interactions, but with different transport coefficients:

$$\mu = \left(\frac{4\alpha}{\pi}+1\right)\hat{P}_1 - (1+\alpha), \qquad \nu = [4(\alpha+1-\hat{P}_2)]^{-1},$$
$$\gamma = \nu\frac{4\alpha}{\rho}\left[\hat{P}_2 - \frac{2}{3\pi}\hat{P}_1\right], \qquad \kappa = \nu\frac{4\alpha}{\rho}\left[\hat{P}_2 + \frac{2}{3\pi}\hat{P}_1\right],$$
$$\xi = \nu\left[\frac{4\alpha}{\rho}\right]^2\frac{1}{3\pi}\hat{P}_1\hat{P}_2. \quad (10)$$

Note first that, contrary to the metric case, the coefficient μ of the linear term does *not* depend on the local density ρ; coefficients of the nonlinear terms depend on density to compensate the density dependence of $\mathbf{w}$. Note further that ν, κ, and ξ are positive since $0<\hat{P}_k<1$, so that, in particular, the nonlinear cubic term is always stabilizing. For an easier discussion, we consider now the Gaussian distribution $P_\sigma(\eta) = \frac{1}{\sigma\sqrt{2\pi}}\exp[-\frac{\eta^2}{2\sigma^2}]$ for which $\hat{P}_k = \exp[-k^2\sigma^2/2]$. Then μ is negative for large σ (where the trivial $\mathbf{w}=0$ solution is stable with respect to linear perturbations), and changes sign for σ_c defined by [27]

$$\sigma_c^2 = 2\ln\left(\frac{1+4\alpha/\pi}{1+\alpha}\right). \quad (11)$$

For $\sigma<\sigma_c$, the nontrivial homogeneous solution $\rho=\rho_0$, $\mathbf{w}=\mathbf{w}_1 \equiv \mathbf{e}\sqrt{\mu/\xi}$ (where $\mathbf{e}$ is an arbitrary unit vector) exists and is stable to homogeneous perturbations.

We now focus on the linear stability of $\mathbf{w}_1$ with respect to an arbitrary wave vector $\mathbf{q}$. Because we want to discuss differences between the metric and metric-free cases later, we keep a formal ρ dependence of the linear transport coefficient. Linearization around $\mathbf{w}_1$ yields

$$\partial_t\delta\rho = -\nabla\cdot\delta\mathbf{w}$$
$$\partial_t\delta\mathbf{w} = -\gamma(\mathbf{w}_1\cdot\nabla)\delta\mathbf{w} - \tfrac{1}{2}\nabla\delta\rho + \nu\nabla^2\delta\mathbf{w} + \kappa\nabla(\mathbf{w}_1\cdot\delta\mathbf{w}) - \kappa\mathbf{w}_1(\nabla\cdot\delta\mathbf{w}) - 2\xi\mathbf{w}_1(\mathbf{w}_1\cdot\delta\mathbf{w}) + (\mu' - \xi'\mathbf{w}_1^2)\mathbf{w}_1\delta\rho, \quad (12)$$

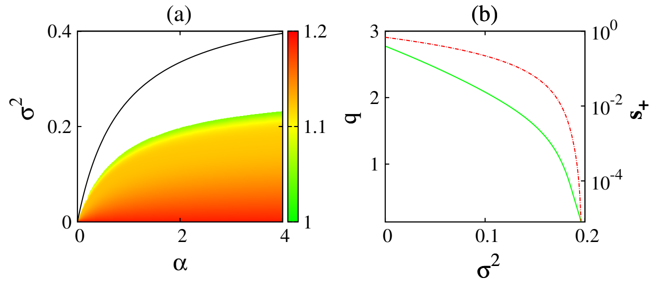

FIG. 1 (color online). Continuous theory for self-propelled particles aligning ferromagnetically [Eqs. (7) and (9) with the coefficients of Eq. (10), Gaussian noise]. (a) Phase diagram in the (α, σ^2) plane. The solid line marks the order-disorder transition. The homogeneous ordered solution $\mathbf{w}_1$ exists below this line and is linearly stable above the colored linear instability region. The color (or gray) scale (in radians) indicates the most unstable wave vector direction ϕ. (b) Modulus q of the most unstable wave vector (green full line) and the real part of its corresponding eigenvalue s_+ (dashed red line) as a function of σ^2 at $\alpha=2$.

where primes indicate derivation with respect to ρ. Using the ansatz $(\delta\rho(\mathbf{r},t), \delta\mathbf{w}(\mathbf{r},t)) = \exp(st + i\mathbf{q}\cdot\mathbf{r})(\delta\rho_\mathbf{q}, \delta\mathbf{w}_\mathbf{q})$ allows us to recast Eq. (12) as an eigenvalue problem for s.

We have solved numerically this cubic problem for the metric-free case using the coefficients of Eq. (10) and Gaussian noise in the full (α, σ) parameter plane. The resulting stability diagram, presented in Fig. 1, shows that, contrary to the metric case, the homogeneous ordered phase is stable near onset. As in the metric case [28], there exists an instability region to oblique wave vectors of large modulus rather far from the transition line. Given that microscopic simulations show no sign of similar instabilities, we believe that the existence of this region, situated away from the validity domain of our approximations, is an artifact of our truncation ansatz.

At the nonlinear level, we performed numerical simulations [29] of Eq. (9) (again with the coefficients of Eq. (10) and Gaussian noise) starting from initial conditions with large variations of both ρ and $\mathbf{w}$. With parameters α and σ^2 in the ordered stable region of Fig. 1, we always observed relaxation towards the linearly stable homogeneous solution $\mathbf{w}_1$, albeit after typically long transients. Starting in the unstable region, the solution blows up in finite time, signaling that indeed our equation is ill behaved when considered too far away from onset.

The stabilization of the near-threshold region by metric-free interactions can be directly traced back to the absence of ρ dependence of μ, in agreement with remarks in Refs. [12,30] where the long-wavelength instability of $\mathbf{w}_1$ was linked to $\mu'>0$. In the long-wavelength limit $q=|\mathbf{q}|\ll 1$, the eigenvalue problem can be solved analytically with relative ease. The growth rate s is the solution of the cubic equation

$$s^3 + \beta_2 s^2 + \beta_1 s + \beta_0 = 0, \quad (13)$$

where the coefficients, to lowest orders in q, are given by

$$\beta_2 = 2\mu + 2iq\sqrt{\frac{\mu}{\xi}}\gamma\cos\phi + 2q^2\nu$$

$$\beta_1 = iq\sqrt{\frac{\mu}{\xi}}\cos\phi\left[2\gamma\mu + \left(\mu' - \mu\frac{\xi'}{\xi}\right)\right] + q^2\left[2\mu\nu + \frac{1}{2} - \frac{\mu}{\xi}(\gamma^2\cos^2\phi + \kappa^2\sin^2\phi)\right]$$

$$\beta_0 = \mu q^2\left[\left(\frac{\mu\xi'}{\xi^2} - \frac{\mu'}{\xi}\right)(\gamma\cos^2\phi + \kappa\sin^2\phi) + \sin^2\phi\right] + iq^3\sqrt{\frac{\mu}{\xi}}\cos\phi\left[\left(\mu' - \mu\frac{\xi'}{\xi}\right)\nu + \frac{\gamma}{2}\right] \quad (14)$$

and ϕ is the angle between $\mathbf{q}$ and $\mathbf{w}_1$ (which has been chosen parallel to the abscissa). Near threshold, where our truncation is legitimate and $\mu \sim \epsilon^2$, two eigenvalues are always stable and linear stability is controlled by the dominant solution real part

$$s_+ \approx \frac{q^2\cos^2\phi}{8\mu}\left[\frac{(\mu')^2}{\mu\xi} - h(\phi)\right] + \mathcal{O}\left(\frac{q^2\mu'}{\mu}\right) \quad (15)$$

with $h(0) = 2$ and $h(\phi) = 1$ otherwise [31]. This expression immediately shows that $s_+ < 0$ in the metric-free case where $\mu' = 0$, confirming the stability of the homogeneous ordered solution $\mathbf{w}_1$. This stabilizing effect can be ultimately traced back to the (negative) pressure term $-\nabla\rho$ appearing in Eq. (9). Conversely, in the metric case for which $\mu \sim 0^+$ near threshold, s_+ is always positive, yielding the generic long-wavelength instability leading to density segregation in metric models.

These results rest on the independence of the linear coefficient μ on ρ, a direct consequence of the fact that the interaction rate per particle in topological models is fixed only by geometrical constraints and does not grow with local density. This property actually holds for any metric-free system: all the linear coefficients μ_k appearing in the equations for $\hat{f}_k$ read

$$\mu_k = \hat{P}_k - 1 - \alpha + \alpha\hat{P}_k(J_{kk} + J_{k0}) \quad (16)$$

and are thus independent of ρ. Therefore, the lack of near-threshold spontaneous segregation extends to the other known classes of "dry" active matter [32]: we have in particular worked out the case of polar particles with nematic alignment ("self-propelled rods") for which $\Psi(\theta_1, \theta_2) = \arg(e^{i\theta_1} + \mathrm{sign}[\cos(\theta_1 - \theta_2)]e^{i\theta_2})$. While full details will be given in Ref. [33], we only sketch here the salient points. Let us first recall that with nematic alignment, the metric model studied at the microscopic level in [9] shows global nematic order. In a large region of parameter space bordering onset, order is segregated to a high-density stationary band oriented along it. We have studied numerically the metric-free version of that Vicsek-style model with Voronoi neighbors. As for its ferromagnetic counterpart, no segregation in bands is observed anymore, and the transition to nematic order is then continuous, as testified by finite-size scaling results (Fig. 2).

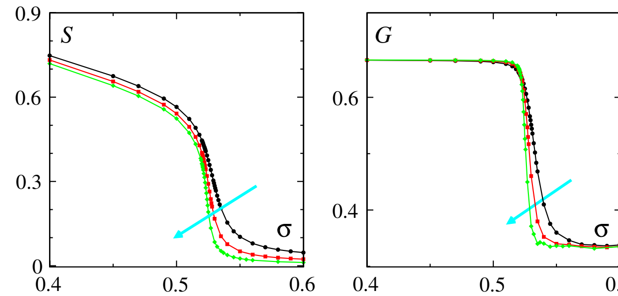

FIG. 2 (color online). Vicsek-style model with nematic alignment and topological neighbors, where $N = L^2$ particles move at a speed $v_0 = \frac{1}{2}$ on a $L \times L$ torus. Headings and positions are updated at discrete time steps according to $\theta_j^{t+1} = \arg[\sum_{k\sim j}\mathrm{sgn}[\cos(\theta_k^t - \theta_j^t)]e^{i\theta_k^t} + n_j^t\sigma\xi_j^t]$ and $\mathbf{r}_j^{t+1} = \mathbf{r}_j^t + v_0\mathbf{e}(\theta_j^{t+1})$, where $\mathbf{e}(\theta)$ is the unit vector along θ, the sum is over the n_j^t Voronoi neighbors of particle j (including j itself), and ξ_j^t is a random unit vector in the complex plane. Nematic order parameter $S = \langle\varphi(t)\rangle_t$ (with $\varphi(t) = |\frac{1}{N}\sum_k e^{i2\theta_k^t}|$) (a) and its Binder cumulant [36] $G = 1 - \langle\varphi(t)^4\rangle_t/(3\langle\varphi(t)^2\rangle_t^2)$ (b) vs σ for $L = 32, 64, 128$ (the arrows indicate increasing sizes). The noncrossing S curves and the absence of minima in the Binder curves all point to a continuous transition. Accurate estimates of its critical exponents will be provided elsewhere.

These properties are well captured, both in the metric and metric-free case, by a controlled hydrodynamic approach of the type presented here, which we only sketch below [33]. The nematic symmetry of the problem requires us to consider three hydrodynamic fields [15], corresponding to the modes $k = 0, 1, 2$ in Eq. (5), with $\hat{f}_2$ coding for the nematic tensor field $\rho\mathbf{Q}$. We have performed the analysis of the 5×5 linear problem expressing the stability of the homogeneous nematically ordered solution ($\mathbf{w} = 0$, $\rho\mathbf{Q} = \text{const}$) appearing at onset in both the metric and nonmetric cases [33]. Whereas the metric case shows a long-wavelength, transversal instability of the homogeneous ordered solution near onset, this solution is linearly stable in the metric-free case. Again, this difference can be traced back to the ρ dependence of the linear coefficients μ_k. At the nonlinear level, simulations indicate that the homogeneous ordered solution is a global attractor in the metric-free case.

Our analysis can also be extended to diffusive active matter such as the driven granular rods model ("active nematics") studied in Refs. [10,11] which, for metric interactions, also shows near-threshold phase segregation [10,34]. Simulations of the metric-free microscopic version (with Voronoi neighbors) show no such segregation. In a kinetic approach, because active nematic particles move by nonequilibrium diffusive currents rather than by ballistic motion, the Boltzmann equation has to be replaced by a more general master equation. But it is nevertheless possible to derive a continuous theory which, in the metric-free case, yields a homogeneous ordered phase stable near onset for essentially the same reasons as in the cases presented above [35].

In conclusion, simple, Vicsek-style, models of active matter where self-propelled particles interact with neighbors defined via nonmetric rules (e.g., Voronoi neighbors) are amenable, like their "metric" counterparts, to the construction of continuous hydrodynamic theories well controlled near onset. The relatively simple framework of Vicsek-style models offers a two-dimensional parameter plane which can be studied entirely. More complicated microscopic starting points, for instance where positional diffusion would also be considered, inevitably raise the dimensionality of parameter space. We have shown here that nonmetric theories differ essentially from metric ones in the independence of their linear coefficients μ_k on the local density, a property directly linked to the fact that the collision rate per particle is constant in metric-free systems. We have shown further that the homogeneous ordered phase is linearly stable near onset for metric-free systems, in contrast with the long-wavelength instability present in metric cases.

We finally discuss the relevance (say in the renormalization-group sense) of metric-free interactions in deciding active matter universality classes. Our work has shown that the deterministic continuous theories of metric-free active matter systems are formally equivalent to those of their metric counterparts, except for the density dependence of the linear coefficients. In the polar case, our hydrodynamic equations thus share the same structure as the Toner and Tu equations [3]. This could be taken as an indication that the homogeneous, ordered, fluctuating phase observed in the Vicsek model with Voronoi neighbors does *not* differ from the Toner-Tu phase of its metric counterpart, in disagreement with the slight numerical discrepancies between the two cases reported in Ref. [23] about the scaling exponent of the anomalously strong density fluctuations. This calls for more extensive microscopic simulations assessing finite-size effects, but also for incorporating effective noise terms, properly derived in both cases, and for studying the resulting field theories, a task left for future work.

We are grateful to I. Giardina, M. C. Marchetti, J. Prost, and J. Toner for enlightening discussions. This work was initiated in the lively atmosphere of the Max Planck Institute for the Physics of Complex Systems in Dresden, Germany, within the Advanced Study Group 2011/2012: Statistical Physics of Collective Motion. F. G. acknowledges support by Grant IIT-Seed Artswarm.

[1] S. Ramaswamy, Annu. Rev. Condens. Matter Phys. **1**, 323 (2010).
[2] T. Vicsek, A. Czirok, E. Ben-Jacob, I. Cohen, and O. Shochet, Phys. Rev. Lett. **75**, 1226 (1995).
[3] J. Toner and Y. Tu, Phys. Rev. Lett. **75**, 4326 (1995); Phys. Rev. E **58**, 4828 (1998); J. Toner, Phys. Rev. Lett. **108**, 088102 (2012).
[4] J. Toner, Y. Tu, and S. Ramaswamy, Ann. Phys. (Berlin) **318**, 170 (2005); P. Romanczuk *et al.*, Eur. Phys. J. Special Topics, **202**, 1 (2012).
[5] D. J. Sumpter, *Collective Animal Behavior* (Princeton University Press, Princeton, NJ, 2010); J. Buhl, D. J. T. Sumpter, I. D. Couzin, J. J. Hale, E. Despland, E. R. Miller, and S. J. Simpson, Science **312**, 1402 (2006).
[6] H. P. Zhang, A. Beer, L. Florin, and H. L. Swinney, Proc. Natl. Acad. Sci. U.S.A. **107**, 13 626 (2010).
[7] J. K. Parrish, S. V. Viscido, and D. Gruñbaum, Biol. Bull. **202**, 296 (2002), and references therein.
[8] G. Grégoire and H. Chaté, Phys. Rev. Lett. **92**, 025702 (2004); H. Chaté, F. Ginelli, G. Gregoire, and F. Raynaud, Phys. Rev. E **77**, 046113 (2008).
[9] F. Ginelli, F. Peruani, M. Bär, and H. Chaté, Phys. Rev. Lett. **104**, 184502 (2010).
[10] H. Chaté, F. Ginelli, and R. Montagne, Phys. Rev. Lett. **96**, 180602 (2006).
[11] S. Ramaswamy, R. A. Simha, and J. Toner, Europhys. Lett. **62**, 196 (2003); S. Mishra and S. Ramaswamy, Phys. Rev. Lett. **97**, 090602 (2006).
[12] E. Bertin, M. Droz, and G. Grégoire, Phys. Rev. E **74**, 022101 (2006); J. Phys. A **42**, 445001 (2009).
[13] T. Ihle, Phys. Rev. E **83**, 030901 (2011).
[14] T. B. Liverpool and M. C. Marchetti, Phys. Rev. Lett. **90**, 138102 (2003); A. Ahmadi, M. C. Marchetti, and T. B. Liverpool, Phys. Rev. E **74**, 061913 (2006).
[15] A. Baskaran and M. C. Marchetti, Phys. Rev. Lett. **101**, 268101 (2008); Phys. Rev. E **77**, 011920 (2008).
[16] V. Narayan, S. Ramaswamy, and N. Menon, Science **317**, 105 (2007).
[17] J. Deseigne, O. Dauchot, and H. Chaté, Phys. Rev. Lett. **105**, 098001 (2010).
[18] V. Schaller, C. Weber, C. Semmrich, E. Frey, and A. R. Bausch, Nature (London) **467**, 73 (2010).
[19] Y. Sumino, K. H. Nagai, Y. Shitaka, D. Tanaka, K. Yoshikawa, H. Chaté, and K. Oiwa, Nature (London) **483**, 448 (2012).
[20] Ballerini *et al.*, Proc. Natl. Acad. Sci. U.S.A. **105**, 1232 (2008).
[21] M. Moussaïd, D. Helbing, and G. Theraulaz, Proc. Natl. Acad. Sci. U.S.A. **108**, 6884 (2011).
[22] J. Gautrais *et al.*, PLoS Comput. Biol. (to be published).
[23] F. Ginelli and H. Chaté, Phys. Rev. Lett. **105**, 168103 (2010).
[24] *Mathematical Methods in Kinetic Theory*, edited by C. Cercignani (Plenum, New York, 1990), 2nd ed., and references therein.
[25] F. Rieke, D. Warland, R. de Ruyter van Steveninck, and W. Bialek, *Spikes: Exploring the Neural Code* (MIT, Cambridge, MA, 1997).
[26] The diffusive ansatz ($\nabla \sim \epsilon$, $\partial_t \sim \epsilon^2$) should be preferred in problems dominated by positional diffusion such as mixtures of filaments, molecular motors, and crosslinking proteins. See I. S. Aranson, and L. S. Tsimring, Phys. Rev. E **71**, 050901(R) (2005); Phys. Rev. E **74**, 031915 (2006); F. Ziebert, I. S. Aranson, and L. S. Tsimring, New J. Phys. **9**, 421 (2007).
[27] While we are considering the small interaction rate limit, α is not necessarily smaller than 1 in the units chosen, for which $v_0 = \lambda = 1$.
[28] In the metric case, this region of instability was overlooked in Ref. [12].

[29] We used a pseudospectral code with Euler time stepping ($\Delta t = 0.01$), with at least 256×256 Fourier modes on square domains of linear size $L = 64$ and antialiasing truncation.
[30] A. Gopinath, M. F. Hagan, M. C. Marchetti, and A. Baskaran, Phys. Rev. E **85**, 061903 (2012).
[31] For $\phi = \pm\pi/2$, one has to resort to higher orders, and then finds $s_+ \approx q^2(-(\mu'/\mu)\kappa\xi + 2\kappa^2\xi - 4\nu\xi^2 + \kappa\xi')/(8\xi^2)$. This quantity is always negative for the coefficients of Eq. (10).
[32] Here we only discuss "dry" systems, where active particles move over a passive background which acts as a momentum sink so that total momentum is not conserved and hydrodynamic long range interactions are ruled out.
[33] A. Peshkov *et al.*, arXiv:1207.5751.
[34] X. Shi and Y. Ma, arXiv:1011.5408.
[35] F. Ginelli *et al.* (to be published).
[36] K. Binder, Rep. Prog. Phys. **60**, 487 (1997).